Cite as:
Luque J., Straub D. (2016). Reliability analysis and updating of deteriorating structural systems with dynamic Bayesian networks. *Structural Safety*, **62**: 34–46

Reliability Analysis and Updating of Deteriorating Systems with Dynamic Bayesian Networks

Jesus Luque & Daniel Straub

Engineering Risk Analysis Group, Technische Universität München (jesus.luque@tum.de, straub@tum.de, www.era.bgu.tum.de)

Abstract

To estimate and update the reliability of deteriorating structural systems with inspection and monitoring results, we develop a modeling and computational framework based on dynamic Bayesian networks (DBNs). The framework accounts for dependence among deterioration at different system components and for the complex structural system behavior. It includes the effect of inspection and monitoring results, by computing the updated reliability of the system and its components based on information from the entire system. To efficiently model dependence among component deterioration states, a hierarchical structure is defined. This structure facilitates Bayesian model updating of the components in parallel. The performance of the updating algorithm is independent of the amount of included information, which is convenient for large structural systems with detailed inspection campaigns or extensive monitoring. The proposed model and algorithms are applicable to a wide variety of structures subject to deterioration processes such as corrosion and fatigue, including offshore platforms, bridges, ships, and aircraft structures. For illustration, a Daniels system and an offshore steel frame structure subjected to fatigue are investigated. For these applications, the computational efficiency of the proposed algorithm is compared with that of a standard Markov Chain Monte Carlo algorithm and found to be orders of magnitude higher.

Keywords

Bayesian analysis; System reliability analysis; Deterioration; Inspection; Fatigue.

1 Introduction

Engineering structures are commonly subjected to deterioration processes, which can reduce their service life and affect the safety of the environment, people and the structure itself. For this reason, significant resources are invested to identify, model, quantify, mitigate and prevent deterioration processes in structures (Swanson 2001, Brownjohn 2007, Farrar and Worden 2007). Structural deterioration, such as metal corrosion and fatigue, is mathematically represented using mostly empirical or semi-empirical models (e.g. Stephens 2001, Gardiner and Melchers 2003, Qin and Cui 2003, Wells and Melchers 2014). Because of their empirical nature, predictive deterioration models are typically associated with significant uncertainty. Hence deterioration is ideally modeled probabilistically (e.g. Madsen et al. 1985, Lin and Yang 1985, Melchers 1999, Frangopol et al. 2004).

Probabilistic deterioration models are developed mainly at the structural component level. However, deterioration at different locations in a structural system is typically correlated, and system considerations should be made (Moan and Song 2000, Vrouwenvelder 2004, Straub and Faber 2005). Probabilistic models of deterioration in large structural systems have been proposed and applied to different types of structures and deterioration processes (e.g. Guedes Soares and Garbatov 1997, Kang and Song 2010, Straub 2011b, Luque et.al 2014, Schneider et al. 2015).

Bayesian methods have been used to combine probabilistic deterioration models with inspection and monitoring outcomes (e.g., Tang 1973, Madsen et al. 1985, Maes et al. 2008, Straub 2009). They allow quantifying the impact of inspections and monitoring on the reliability of the structure, and so facilitate maintenance decisions and the planning of future inspections (e.g. Thoft-Christensen and Sørensen 1987, Faber et al. 2000, Moan 2005, Straub and Faber 2005). Bayesian analysis is mainly performed at the component level, where the probability of failure of a structural component due to deterioration is updated with the inspection and monitoring outcomes. Only a few publications consider the updating of the reliability at the structural system level. Therein, the dependence among component deterioration states is modeled either through the correlation among the deterioration limit states (Moan and Song 2000, Lee and Song 2014, Maljaars and Vrouwenvelder 2014) or through a hierarchical model (Mahadevan 2001, Faber et al. 2006, Maes and Dann 2007, Straub et al. 2009, Schneider et al., under review). More recently, a number of researchers have considered the planning and optimization of inspection and maintenance actions in structural systems with dependent component deterioration (Straub and Faber 2005, Qin and Faber 2012, Nielsen and Sørensen 2014, Memarzadeh et al. 2014).

A challenge in Bayesian system reliability analysis is to keep the computation time at a feasible level. Methods belonging to classical structural reliability methods are efficient for estimating the probability of system failure, but do not facilitate Bayesian analysis or have computation times that increase exponentially with the number of observations. Recently, a class of methods has been proposed that efficiently combine structural reliability methods with Bayesian updating (Straub 2011a, Straub and Papaioannou 2015). Nevertheless, also this approach has the drawback that its performance is a function of the number of inspection and monitoring data, which can be considerable in structural systems.

Bayesian Networks (BNs) have become popular in engineering risk analysis due to their intuitive nature and their ability to handle many dependent random variables in a Bayesian analysis (Jensen and Nielsen 2007, Straub and Der Kiureghian 2010, Weber et al. 2010). The graphical structure of the BN is formed by nodes and directed links. The nodes represent random variables or deterministic parameters, and the links the dependence among nodes. Ideally, the link between two nodes is based on a causal relation, but this is not necessary. As an example, if deterioration D is modeled as a function of an external random load S and a material parameter M, then a corresponding BN may look like the one in Figure 1. Here, an additional node Z is included, representing an outcome of an inspection. Since each random variable in the BN is specified by its conditional probability distribution given its parents, the inspection outcome is defined by $p(z|d)$, i.e. the probability of the inspection outcome $Z = z$ given the damage state $D = d$. This is known as the likelihood function, and corresponds to classical models used for describing inspection or monitoring performance, such as Probability of Detection (POD). Generally, the BN is established using commonly available probabilistic models; it allows combining these in a consistent and (in most cases) intuitive manner.

Using BNs it is possible to obtain the posterior distribution of a set of random variables given a set of observations. This task is called inference. For instance, if an inspection result is included in the previously presented example, i.e. if Z is given, then the (joint) probability distribution of the random variables S, M and D conditional on the observed value of Z is calculated using inference algorithms. There are many algorithms available for inference in BNs (e.g. Hanea et al. 2006, Langseth 2009, Shenoy and West 2011). In this paper, the focus is on BN with discrete random variables, for which exact inference algorithms exist (e.g. Murphy 2002, Jensen and Nielsen 2007).

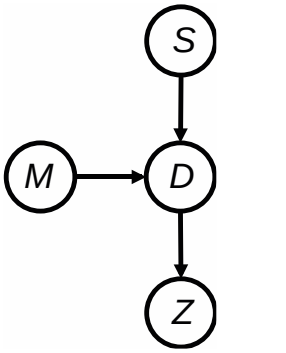

Figure 1. BN deterioration model example.

The links in the BN provide information on the dependence between random variables in the model. For example, in the BN of Figure 1, M and S are assumed to be independent a-priori, and hence no direct link between them is present. The link from D to Z indicates that the inspection provides information on the damage state. It provides no direct information on S and M. However, it does so indirectly, because the information obtained on D also updates the probability distribution of S and M, as long as D is not known with certainty. In this way, by observing one random variable, potentially all others are updated. However, for efficient computation, all BN inference algorithms make use of the graphical structure by performing computations locally, exploiting the conditional independence assumptions encoded in the graph.

Modeling of deterioration often involves random processes, which can be represented in a discrete-time manner by dynamic Bayesian networks (DBN), as proposed in Straub (2009). For illustration, we extend the BN of Figure 1 to include a time-variant load S_t and inspection results at multiple points in time $t = 1, \dots, T$. The resulting DBN is shown in Figure 2. Each "slice" of the DBN represents a time step in the analysis. The random process $\{S_1, S_2, \dots, S_T\}$ is a Markov chain where each random variable is defined conditionally on the random variables of the previous time step. The deterioration D_t at time t is a stochastic function of the previous deterioration state D_{t-1} and the current load S_t. The probability distributions of the material parameter M, the loads $\{S_1, S_2, \dots, S_T\}$, and the deterioration states $\{D_1, D_2, \dots, D_T\}$ are all updated once inspection outcomes Z_1, …, Z_T, or a subset thereof, are observed.

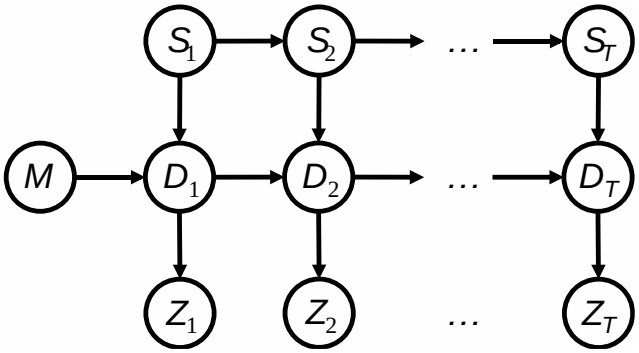

Figure 2. DBN deterioration model example.

In this paper, the DBN model for structural deterioration from Straub (2009) is extended from the component to the system level, based on work presented by the authors in Luque and Straub (2015). An efficient algorithm is developed, which assesses the reliability of a deteriorating system when partial observations of its condition are available. The deterioration factors of the system components are interrelated using a hierarchical structure and a set of hyperparameters, which model the correlation structure among components. In the following section, the concept of dynamic Bayesian networks and its application to efficiently model component deterioration are presented. Thereafter, in Section 3, the model is extended to represent the complete structural system. Sections 4.1 and 4.2 present two case studies where the model and algorithm are applied and compared to other methods for estimating the system probability of failure. To demonstrate the advantages of the proposed algorithm, the number of system components is increased to a point where classical MCMC algorithms are no longer efficient for estimating the system reliability.

2 Dynamic Bayesian network for assessing component deterioration

2.1 DBN model of a single component

The DBN model framework developed in Straub (2009) is used to represent the deterioration of components. This model includes the following elements:

- Time-invariant model parameters $\boldsymbol{\theta}$, which are constant in time.
- Time-variant model parameters $\boldsymbol{\omega}_t$, which vary with time steps $t = 0, \dots, T$.
- Deterioration model: A parametric function h for describing the deterioration D as a function of t, $\boldsymbol{\theta}$, $\boldsymbol{\omega}_0, \dots, \boldsymbol{\omega}_t$ and the deterioration level at the previous time step D_{t-1}, i.e.

$$D_t = D(t) = h(t, D_{t-1}, \boldsymbol{\theta}, \boldsymbol{\omega}_1, \ldots, \boldsymbol{\omega}_t), \quad t = 1, \ldots, T \tag{1}$$

- Observations: At any time step t, information on the condition of a model parameter or the deterioration D_t may be available from inspections, monitoring systems, recordings of environmental parameters or other measurements, which are related to the model parameters. These observations are denoted by $Z_{\boldsymbol{\theta},t}$, $Z_{\boldsymbol{\omega},t}$, and $Z_{D,t}$, depending on the random variables to which they relate.

Figure 3 depicts the generic DBN deterioration model for a single component, where vectors $\boldsymbol{\theta}_1, \ldots, \boldsymbol{\theta}_T$ are added in order to have a repetitive sub-BN for each time step. These vectors are deterministically defined as $\boldsymbol{\theta}_t = \boldsymbol{\theta}_{t-1} = \boldsymbol{\theta}_0$ for all $t = 1, \ldots, T$. The DBN model illustrates how the parameters and the deterioration of a single component are related in time. Each set $\{\boldsymbol{\theta}_t, \boldsymbol{\omega}_t, D_t, Z_{\boldsymbol{\theta},t}, Z_{\boldsymbol{\omega},t}, Z_{D,t}\}$ represents a time step t in the DBN.

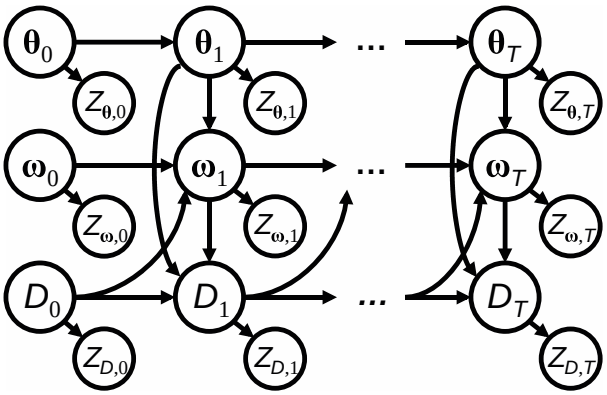

Figure 3. Generic DBN of the deterioration model at the component level (following Straub 2009).

2.2 Computation of the posterior distribution

DBN models can be evaluated using exact or approximate inference algorithms. Most approximate methods are sampling-based; the most popular among these belong to the family of Markov Chain Monte Carlo (MCMC) methods. MCMC using Gibb's sampler is particularly effective, as it exploits the conditional independence properties of the BN (Gamerman and Lopes 2006). Nevertheless, the computational cost of MCMC increases considerably as the number of observations included in the model increases and/or the probability of failure of interest decreases. This motivates the use of exact inference algorithms with discretized random variables, whose performance does not deteriorate with increasing amount of observation and is independent of the magnitude of the probabilities of interest.

For DBN models consisting exclusively of discrete random variables, exact inference algorithms exist. In particular the forward-backward algorithm (Murphy 2002, Russell and Norvig 2003) is effective for DBN. In Straub (2009), a variant of the forward-backward algorithm is proposed, which is tailored towards evaluating the generic DBN for deterioration modeling shown in Figure 3.

2.3 Discretization of continuous random variables

With the exception of some special cases, exact inference algorithms can be applied only to DBNs with exclusively discrete random variables. However, most deterioration models include continuous random variables. To apply the exact inference algorithms, these must be discretized. To this end, the original continuous domain of each random variable is partitioned into discrete intervals and the probability of each interval is computed from the conditional or the marginal PDF of the random variable. Even though these algorithms are exact for a given discretization, the discretization itself does introduce an error. The number and location of the discrete intervals have an impact on the computation time and accuracy of the approximation. Several algorithms have been developed to obtain optimal intervals based on a specific estimation, typically the probability of failure (Chang and Chen 2005, Neil et al. 2007, Marquez et al. 2010, Zwirglmaier and Straub under review).

Here the heuristic principles presented in Straub (2009) to define the discretization scheme are used. To keep the model simple, the discretization scheme, and hence the conditional probabilities, are the same in all time steps, resulting in a homogenous DBN. The discretization scheme of the random variables $\boldsymbol{\theta}$ and $\boldsymbol{\omega}_t$ is chosen so that after applying the deterioration model h, they result in approximately equally spaced intervals in D. This method is simple to implement and has proven to be effective. For more details on discretization approach, the reader is referred to Straub (2009).

3 Bayesian network model of system deterioration

One challenging aspect of modeling deteriorating structural systems is the representation of the interrelation among the system components and the common factors that affect their condition. Only a limited number of investigations of the dependence among component deterioration states can be found in the literature (e.g. Hergenröder and Rackwitz 1992, Vrouwenvelder 2004, Maes et al. 2008, Malioka 2009, Luque et.al 2014). The two most common mathematical representations of such dependence are hierarchical models and random field models. The latter

are suitable for systems where dependence among component deterioration is a function of the geometrical location (Maes 2003, Stewart and Mullard 2006). Hierarchical models are suitable where the dependence among component deterioration depends on common features and common influencing factors (Maes and Dann 2007, Maes et al. 2008, Banerjee et al. 2015). They have computational advantages over random fields, in particular in the context of DBN modeling.

In the DBN model, care is required to correctly represent the statistical dependence among the random variables without increasing the complexity and computational cost of the inference. For general statistical dependence among components, most DBN models of systems rapidly become computationally intractable when the number of components in the system or the number of random variables increases. Strategies for reducing the computational efforts when representing random fields in the BN have been proposed (Bensi et al. 2011), but their applicability is still limited. In the proposed approach, the dependence structure is modeled by hierarchical models. Hierarchical models can capture the dependence structure of deterioration in most structural systems quite adequately, because the dependence is typically caused mainly by common influencing factors rather than geometrical proximity.

3.1 Hierarchical models

Hierarchical models are an effective way of representing systems whose characteristics can be grouped using multiple levels (Raudenbush and Bryk 2008). The random variables within a level are interrelated through common influencing parameters, which are modeled at a higher level in the hierarchy. The random variables at the highest level are called hyperparameters. As a simple example, Figure 4 shows a BN representing a set of random variables $\{V_1, V_2, \dots, V_n\}$ with common mean value α. As long as the value of α is uncertain, the random variables $\{V_1, V_2, \dots, V_n\}$ are statistically dependent. The correlation between V_i and V_j will depend on the distribution parameters. If the random variables V_i conditional on α all have standard deviation σ_V, and α has standard deviation σ_0, then the linear correlation between any pair V_i and V_j, $i \neq j$, is

$$\rho(V_i, V_j) = \frac{\sigma_0^2}{\sigma_0^2 + \sigma_V^2} \tag{2}$$

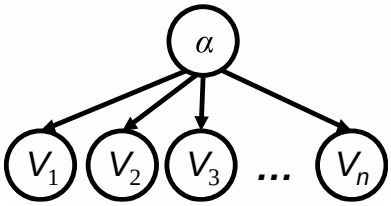

Figure 4. Hierarchical BN with a hyperparameter α.

3.2 Hierarchical model based on correlation models

In many instances, influencing parameters are not modeled explicitly, as in the example above, but instead models of the correlation among components are available. In this section, we describe how such correlation models are translated into a BN. To simplify the presentation, we consider an equi-correlated set of random variables $\mathbf{V} = [V_1, \dots, V_n]^T$, for which the correlation between any two components is ρ_V. All V_i's have identical marginal distribution, described by the cumulative distribution function (CDF), F_V. The extension to more general cases is outlined afterwards. The presentation is limited to the (commonly implied) case that the joint distribution of $\mathbf{V}$ follows a Gaussian copula, i.e. the Nataf transformation can be used for transforming the $\mathbf{V}$ to equivalent standard normal random variables (Liu and Der Kiureghian 1986).

Following the principle of the Nataf transformation, the V_i are related to corresponding standard normal distributed Y_i through the following marginal transformation:

$$V_i = F_V^{-1}[\Phi(Y_i)] \tag{3}$$

where F_V^{-1} is the inverse CDF of V_i and Φ is the standard normal CDF.

The Y_i are jointly normal distributed with correlation coefficient ρ_Y, which is the equivalent correlation in standard normal space and is a function of ρ_V and F_V. Its value is such that, after applying the transformation $F_V^{-1}[\Phi(\cdot)]$, the resulting random variables $V_1, \dots, V_n$ have correlation ρ_V. ρ_Y can be found numerically or from the approximate expressions provided in (Liu and Der Kiureghian 1986).

The dependence among the equi-correlated standard normal random variables $Y_1, \dots, Y_n$ can be defined through a hierarchical structure. To this end, a standard normal hyperparameter α is introduced, as shown in Figure 5. The Y_i are defined as normal random variables conditional on α with mean $\sqrt{\rho_Y} \cdot \alpha$ and standard deviation $\sqrt{1-\rho_Y}$. The unconditional $Y_1, \dots, Y_n$ are then standard normal random variables with mutual correlation coefficient ρ_Y.

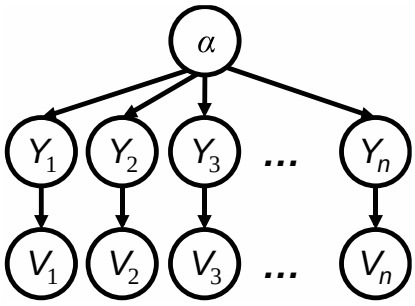

Figure 5. Hierarchical BN of equally correlated random variables.

To reduce the number of random variables in the BN, the auxiliary random variables Y_i can be eliminated and replaced by a direct link between α and the V_i. The resulting BN is the one in Figure 4. The corresponding conditional distribution of V_i given α is:

$$F_{V|\alpha}(v) = \Phi\left(\frac{\Phi^{-1}\left(F_V(v)\right) - \sqrt{\rho_Y}\cdot\alpha}{\sqrt{1-\rho_Y}}\right) \tag{4}$$

The conditional CDF of the random variables V_i of Eq. (4) is used to generate the conditional probability table (CPT) of V_i in the DBN system deterioration model.

The above model approach can be extended to random variables $V_1, \dots, V_n$ with different marginal distributions and varying mutual correlation coefficients. As long as the pairwise correlation coefficients $\rho_{Y,ij}$ of the underlying standard normal $Y_i's$ are of the Dunnett-Sobel class (see e.g. Thoft-Christensen and Murotsu 1986, Kang and Song 2009), the BN structures of Figure 4 and Figure 5 still hold. No additional computational efforts are necessary in these cases.

3.3 DBN model of the system

The hierarchical DBN modeling approach is applied to model dependence among component deterioration in structures. To extend the component DBN model of section 2.1 to a model of the structural system, a set of hyperparameters $\boldsymbol{\alpha} = \left[\alpha_{\boldsymbol{\theta}}, \alpha_{\boldsymbol{\omega}}, \alpha_{D_0}\right]^T$ are defined. In the system model, all components are connected through these hyperparameters $\boldsymbol{\alpha}$ (Figure 6). All random variables in the DBN are now indexed by the component number $i = 1, \dots, N$ and the time step $t = 0, \dots, T$, i.e. $D_{3,10}$ is the damage of component 3 at time step 10.

The $\boldsymbol{\alpha}$ parameters may be determined from known correlation among components, following Section 3.2, or derived from common influencing factors. In many cases, they will represent

model uncertainties, which are typically shared among similar components within a system. In this case, the corresponding $\boldsymbol{\alpha}$ parameters can be obtained by first estimating the magnitude of common model uncertainties relative to component-specific uncertainties, then determining the corresponding correlations through Eq. (2) and from those the $\boldsymbol{\alpha}$ parameters following Section 3.2.

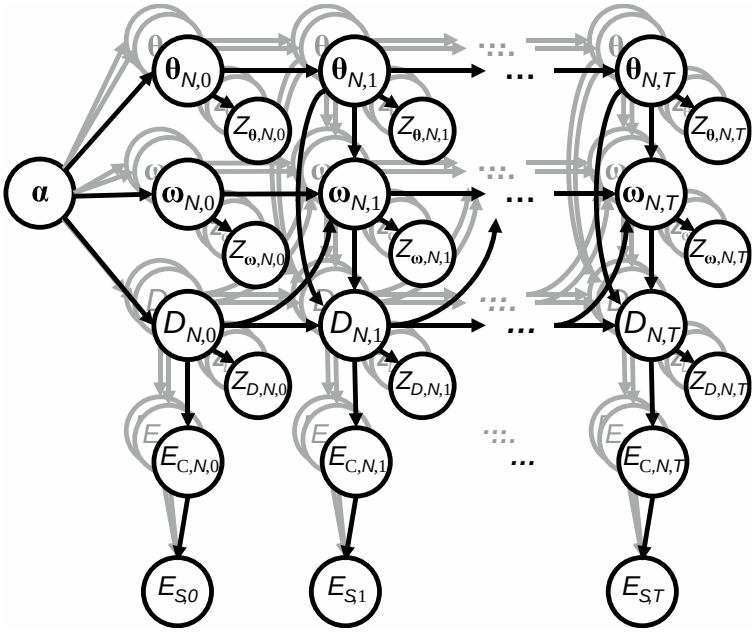

Figure 6. DBN model of the structural system deterioration.

In the full system model DBN of Figure 6, the binary random variable $E_{C,i,t}$ represents the condition (i.e. $E_{C,i,t} = 0$: not failed, $E_{C,i,t} = 1$: failed) of component i at time step t. $E_{C,i,t}$ is a (possibly probabilistic) function of the deterioration state $D_{i,t}$. The binary random variable $E_{S,t}$ represents the system condition (i.e. $E_{S,t} = 0$: not failed, $E_{S,t} = 1$: failed) as a function of all component conditions. $E_{C,i,t}$ and $E_{S,t}$ can be extended to multi-state random variables, if a more detailed description of the components and system condition is desirable. The relation between the system condition $E_{S,t}$ and the condition of its components $E_{C,i,t}$, $i = 1, \dots, N$, is quantified by the probability of system failure given the conditions of its components. To obtain these conditional probabilities, a probabilistic model of the structural system is necessary and structural reliability computations must be performed in a pre-processing step.

For many real structural systems, the number of system components subject to deterioration is large, and hence there is a prohibitively large number of combinations of component deterioration states in the system, as discussed in Straub and Der Kiureghian (2011). In the DBN model of Figure 6, this is reflected by the number of links pointing from the component

condition nodes $E_{C,i,t}$, $i = 1, \dots, N$ to the system condition node $E_{S,t}$. For each combination of possible element conditions, a system configuration $\boldsymbol{\Psi}_t$ is defined. A total of 2^N different system configurations must be examined, which rapidly becomes intractable as the number of components increases, because a system reliability analysis must be carried out for each configuration to determine $\Pr(E_{S,t} = 1 | \boldsymbol{\Psi}_t = \boldsymbol{\psi}_t)$. In specific applications of the framework, it is therefore necessary to use a more efficient representation of structural system behavior. For this purpose, the convergent connection from the $E_{C,i,t}$ to $E_{S,t}$ may be replaced by an alternative dependence structure. Different techniques can be used to this end, in function of the considered system. One possible alternative is to reduce the number of system configurations to consider based on their contribution to the probability of failure (Kim et al. 2013). Alternatively, in many systems one can exploit the fact that some components are (approximately) exchangeable with respect to their static function. In this case, it is sufficient to consider the number of component failures in the group (Straub and Der Kiureghian 2011). In the numerical investigations presented later, we consider a Daniels system to demonstrate the DBN modeling in such cases. Furthermore, in some systems it is possible to pursue a hierarchical modeling approach also for the static functions. Such a strategy is utilized in the second numerical example presented later.

3.4 Inference algorithm

To perform inference with the system DBN, i.e. to compute the probability of component and system failure given inspection and monitoring results, the forward-backward algorithm presented in Straub (2009) for exact inference is extended to the system level. The algorithm presented here is limited to the forward operation, which is used to solve the filtering problem, i.e. to compute the posterior distribution of the random variables $\boldsymbol{\alpha}$, $\boldsymbol{\theta}_i$, $\boldsymbol{\omega}_{i,t}$, $D_{i,t}$, $E_{C,i,t}$ and $E_{S,t}$ for all $i = 1, \dots, N$ given the observations up to time t. The algorithm is formulated in a recursive manner for each time step and exploits the property of the hierarchical model that all components are statistically independent for given hyperparameters.

3.4.1 Component partial updating (forward operation)

This first part of the algorithm is applied to each component separately. The conditional joint probability mass function (PMF) of deterioration state $D_{i,t}$, the time-variant parameters $\boldsymbol{\omega}_{i,t}$, and the time-invariant parameters $\boldsymbol{\theta}_i$ are computed conditionally on the hyperparameters $\boldsymbol{\alpha}$ and on all observations of the component up to time step t. The latter are denoted by $\mathbf{Z}_{i,0:t}$, and include all observations of the damage state $Z_{D,i,0:t}$, time-variant $Z_{\boldsymbol{\omega},i,0:t}$ and time-invariant

parameters $Z_{\boldsymbol{\theta},i,0:t}$, i.e. $\mathbf{Z}_{i,0:t} = \left[Z_{D,i,0:t}, Z_{\boldsymbol{\omega},i,0:t}, Z_{\boldsymbol{\theta},i,0:t}\right]^T$. From application of Bayes' rule, and accounting for the independence properties encoded in the DBN structure, it follows:

$$p\left(d_{i,t}, \boldsymbol{\omega}_{i,t}, \boldsymbol{\theta}_{i,t} \middle| \boldsymbol{\alpha}, \mathbf{z}_{i,0:t}\right)$$

$$\propto p\left(d_{i,t}, \boldsymbol{\omega}_{i,t}, \boldsymbol{\theta}_{i,t} \middle| \boldsymbol{\alpha}, \mathbf{z}_{i,0:t-1}\right) p\left(z_{D,i,t} \middle| d_{i,t}\right) p\left(z_{\boldsymbol{\omega},i,t} \middle| \boldsymbol{\omega}_{i,t}\right) p\left(z_{\boldsymbol{\theta},i,t} \middle| \boldsymbol{\theta}_{i,t}\right) \tag{5}$$

where $i = 1, \dots, N$, $t = 1, \dots, T$. The proportionality constant is found by normalization: $\sum_{d_{i,t}} \sum_{\boldsymbol{\omega}_{i,t}} \sum_{\boldsymbol{\theta}_{i,t}} p\left(d_{i,t}, \boldsymbol{\omega}_{i,t}, \boldsymbol{\theta}_{i,t} \middle| \boldsymbol{\alpha}, \mathbf{z}_{i,0:t}\right) = 1$. The first term on the right hand side of Eq. (5) is calculated from the joint probability at the previous time step $p\left(d_{i,t-1}, \boldsymbol{\omega}_{i,t-1}, \boldsymbol{\theta}_{i,t-1} \middle| \boldsymbol{\alpha}, \mathbf{z}_{i,0:t-1}\right)$ through:

$$p\left(d_{i,t}, \boldsymbol{\omega}_{i,t}, \boldsymbol{\theta}_{i,t} \middle| \boldsymbol{\alpha}, \mathbf{z}_{i,0:t-1}\right)$$

$$= \sum_{d_{i,t-1}} p\left(d_{i,t} \middle| d_{i,t-1}, \boldsymbol{\omega}_{i,t}, \boldsymbol{\theta}_{i,t}\right) \sum_{\boldsymbol{\omega}_{i,t-1}} p\left(\boldsymbol{\omega}_{i,t} \middle| d_{i,t-1}, \boldsymbol{\omega}_{i,t-1}, \boldsymbol{\theta}_{i,t}\right)$$

$$\times \sum_{\boldsymbol{\theta}_{i,t-1}} p\left(\boldsymbol{\theta}_{i,t} \middle| \boldsymbol{\theta}_{i,t-1}\right) p\left(d_{i,t-1}, \boldsymbol{\omega}_{i,t-1}, \boldsymbol{\theta}_{i,t-1} \middle| \boldsymbol{\alpha}, \mathbf{z}_{i,0:t-1}\right) \tag{6}$$

The algorithm is applied recursively, starting at $t = 0$, for which the joint probability is

$$p\left(d_{i,0}, \boldsymbol{\omega}_{i,0}, \boldsymbol{\theta}_{i,0} \middle| \boldsymbol{\alpha}, \mathbf{z}_{i,0}\right)$$

$$\propto p\left(z_{D,i,0} \middle| d_{i,0}\right) p\left(z_{\boldsymbol{\omega},i,0} \middle| \boldsymbol{\omega}_{i,0}\right) p\left(z_{\boldsymbol{\theta},i,0} \middle| \boldsymbol{\theta}_{i,0}\right) p\left(d_{i,0} \middle| \boldsymbol{\alpha}\right) p\left(\boldsymbol{\omega}_{i,0} \middle| \boldsymbol{\alpha}\right) p\left(\boldsymbol{\theta}_{i,0} \middle| \boldsymbol{\alpha}\right) \tag{7}$$

Note that all conditional probabilities required in Eqs. (5-7) are available from the definition of the BN.

3.4.2 Hyperparameter updating

Observations of each component have an indirect effect on the posterior distribution of the remaining components. These distributions are updated through the hyperparameters. For this reason, the second step is updating the hyperparameters given the observations from all random

variables up to time t, i.e. $p(\boldsymbol{\alpha}|\mathbf{z}_{1:N,0:t})$. This is calculated recursively with respect to i (i.e. component by component) as:

$$p(\boldsymbol{\alpha}|\mathbf{z}_{1:i,0:t}) \propto p(\boldsymbol{\alpha}|\mathbf{z}_{1:i-1,0:t}) \prod_{j=0}^{t} p(\mathbf{z}_{i,j}|\boldsymbol{\alpha}) \tag{8}$$

for $i = 2, \dots, N$, and

$$p(\boldsymbol{\alpha}|\mathbf{z}_{1,0:t}) \propto p(\boldsymbol{\alpha}) \prod_{j=0}^{t} p(\mathbf{z}_{1,j}|\boldsymbol{\alpha}) \tag{9}$$

where $p(\boldsymbol{\alpha}|\mathbf{z}_{1:i,0:t})$ is the conditional probability of the hyperparameters given all observations in components $1, \dots, i$ up to time t and $p(\boldsymbol{\alpha})$ is the prior probability of the hyperperameters (i.e. before observations). $p(\mathbf{z}_{i,t}|\boldsymbol{\alpha})$ is the inverse of the normalizing constant of Eq. (5), for component i and time step t. Equation (8) can also be expressed as a product over the index i, but it is expressed in recursive form here to indicate that the conditional probability of the hyperparameters given the observations can be partially calculated after each component is updated.

3.4.3 Posterior distributions

The next step in the algorithm is the computation of the joint posterior probability $p(d_{i,t}, \boldsymbol{\omega}_{i,t}, \boldsymbol{\theta}_{i,t}, \boldsymbol{\alpha}|\mathbf{z}_{1:N,0:t})$, the updated component state probability given the observations from all components up to time t:

$$p(d_{i,t}, \boldsymbol{\omega}_{i,t}, \boldsymbol{\theta}_{i,t}, \boldsymbol{\alpha}|\mathbf{z}_{1:N,0:t}) = p(d_{i,t}, \boldsymbol{\omega}_{i,t}, \boldsymbol{\theta}_{i,t}|\boldsymbol{\alpha}, \mathbf{z}_{i,0:t}) p(\boldsymbol{\alpha}|\mathbf{z}_{\{1:N\}\setminus\{i\},0:t}) \tag{10}$$

where $\mathbf{z}_{\{1:N\}\setminus\{i\},0:t}$ are the observations of all components excluding those of component i. Any marginal posterior distribution can be computed from these results. As an example, the posterior distribution of the damage in component i at time t is:

$$p(d_{i,t}|\,\mathbf{z}_{1:N,0:t}) = \sum_{\boldsymbol{\omega}_{i,t}} \sum_{\boldsymbol{\theta}_{i,t}} \sum_{\boldsymbol{\alpha}} p(d_{i,t}, \boldsymbol{\omega}_{i,t}, \boldsymbol{\theta}_{i,t}, \boldsymbol{\alpha}|\,\mathbf{z}_{1:N,0:t}) \tag{11}$$

3.4.4 Posterior reliability of components and system

Finally, the updated probability of the component condition $E_{C,i,t}$ is obtained by simple application of the total probability theorem:

$$p(e_{C,i,t}|\mathbf{z}_{1:N,0:t}) = \sum_{d_{i,t}} p(e_{C,i,t}|d_{i,t})\, p(d_{i,t}|\mathbf{z}_{1:N,0:t}) \tag{12}$$

where $e_{C,i,t}$ is a realization of the random variable $E_{C,i,t}$. The updated probability distribution of the system condition is:

$$\begin{aligned} & p(e_{S,t}|\mathbf{z}_{1:N,0:t}) \\ &= \sum_{e_{C,1,t},\dots,e_{C,N,t}} p(e_{S,t}|\mathbf{e}_{C,1:N,t}) \sum_{\boldsymbol{\alpha}} p(\mathbf{e}_{C,1:N,t}|\boldsymbol{\alpha}, \mathbf{z}_{1:N,0:t})\, p(\boldsymbol{\alpha}|\mathbf{z}_{1:N,0:t}) \\ &= \sum_{e_{C,1,t},\dots,e_{C,N,t}} p(e_{S,t}|\mathbf{e}_{C,1:N,t}) \sum_{\boldsymbol{\alpha}} p(\boldsymbol{\alpha}|\mathbf{z}_{1:N,0:t}) \prod_{i} p(e_{C,i,t}|\boldsymbol{\alpha}, \mathbf{z}_{1:N,0:t}) \end{aligned} \tag{13}$$

where $\mathbf{e}_{C,1:N,t} = [e_{C,1,t}, \dots, e_{C,N,t}]^T$ is a realization of $\mathbf{E}_{C,1:N,t} = [E_{C,1,t}, \dots, E_{C,N,t}]^T$.

3.5 Computational complexity of the algorithm

The computational complexity of the forward operation for a single component is $O[m_\theta(t+1)(m_D^2 m_\omega + m_D m_\omega^2)]$, where m_D, m_ω, m_θ are the number of states of the discretized random variables $D_{i,t}$, $\boldsymbol{\theta}_{i,t}$, $\boldsymbol{\omega}_{i,t}$ (see Straub 2009). In analogy, the complexity of the algorithm described in section 3.4.1 for updating all components with their respective observations is $O[m_\theta m_\alpha N(t+1)(m_D^2 m_\omega + m_D m_\omega^2)]$, where m_α is the number of states of the hyperparameters. The complexity of the hyperparameter updating step of section 3.4.2 is $O[m_D m_\omega m_\theta m_\alpha N]$. The complexity of updating the condition of all components is $O[m_C m_D N]$ and that of updating the system reliability is $O\left[[(N+1)m_\alpha + 1] m_{E_S} m_{E_C}^N\right]$ in the general case (section 3.4.3).

With the exception of the updating of the system condition E_S, the complexity of the algorithm is proportional to the number of components and time steps and it is independent of the number of observations included in the analysis. However, updating of E_S can quickly become intractable as the number of components increases, unless a more efficient system representation than the convergent connection (Figure 6) can be found. Such strategies were already discussed in section 3.3. Alternatively, if such alternative system representations are

not possible or not convenient, the conditional system reliability may be evaluated using sampling-based structural reliability methods. This could be achieved by employing the conditional probability distributions computed with the DBN algorithm to generate samples from the posterior.

A second important aspect of computational performance is the necessary memory allocation. This is strongly influenced by the size of the largest joint PMF used in the procedure, which can be either $p\left(D_{i,t}, \boldsymbol{\omega}_{i,t}, \boldsymbol{\theta}_{i,t} \middle| \boldsymbol{\alpha}\right)$ or $p\left(\boldsymbol{\omega}_{i,t} \middle| D_{i,t-1}, \boldsymbol{\omega}_{i,t-1}, \boldsymbol{\theta}_{i,t}\right)$. Memory allocation as well as computational complexity are therefore a direct function of the discretization scheme, which must be defined carefully to find an optimal trade-off between accuracy and computational cost.

4 Numerical investigation

The following numerical examples serve to investigate and illustrate the workings of the proposed model and inference algorithm. For validation purposes, the results obtained with the exact inference algorithm are compared to those obtained with two alternative methods: 1) Monte Carlo simulation (MCS) for the case without observations, and 2) MCMC for cases with and without observations. The MCMC computations are implemented with OpenBUGS (Lunn et.al 2009).

4.1 Daniels system

For illustration purposes, we consider a Daniels system (Daniels 1945, Gollwitzer and Rackwitz 1990), which consists of a set of N elements with independent and identically distributed capacities R_i for $i = 1, \dots, N$. The elements have ideally brittle material behavior. The system is subject to a load L (Figure 7).

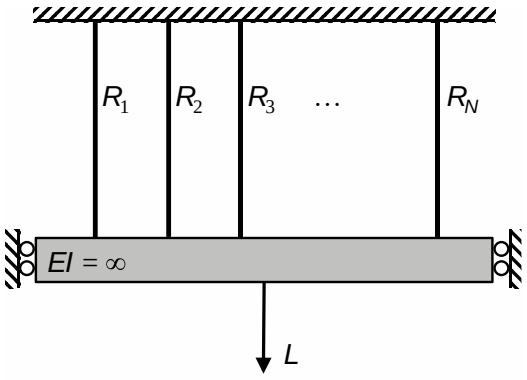

Figure 7. Daniels system.

Prior to the application of the load, each component in the system is in one of two possible states: a) full capacity, or b) zero capacity due to a fatigue failure. For a discussion of this model see Straub and Der Kiureghian (2011).

4.1.1 Deterioration model

The system components are subject to fatigue deterioration, which - for illustration purposes - is modeled by simple fracture-mechanics-based crack growth model (e.g. Ditlevsen and Madsen 1996). It uses Paris' law to describe the growth of the crack depth D_i at component i:

$$\frac{\mathrm{d}D_i(n)}{\mathrm{d}n} = C_i \left[\Delta S_{e,i}\sqrt{\pi D_i(n)}\right]^{M_i} \tag{14}$$

where n = number of stress cycles; $\Delta S_{e,i} = (\mathrm{E}[\Delta S_i^M])^{\frac{1}{M}}$ = equivalent stress range per cycle with $\mathrm{E}[\cdot]$ being the expectation operator; ΔS_i = stress range per cycle; C_i, M_i = empirically determined material parameters.

The long-term distribution of the fatigue stress range ΔS_i is described by a Weibull distribution with scale and shape parameters K_i and λ_i. $\Delta S_{e,i}$ is then given by (Madsen 1997):

$$\Delta S_{e,i} = K_i \Gamma\left(1 + \frac{M_i}{\lambda_i}\right)^{\frac{1}{M_i}} \tag{15}$$

where $\Gamma(\cdot)$ is the Gamma function. Using the initial condition $D_i(n=0) = D_{i,0}$, the following analytical solution for the crack depth after n stress cycles can be obtained from Eq. (14):

$$D_i(n) = \left[\left(1 - \frac{M_i}{2}\right) C_i \Delta S_{e,i}^{M_i} \pi^{M_i/2} n + D_{i,0}^{1-M_i/2}\right]^{(1-M_i/2)^{-1}} \tag{16}$$

4.1.2 Observations and probability of detection

In this example, we only consider observations of the deterioration state through inspections, e.g. visual inspections or non-destructive evaluation of the fatigue hot spots. The observation $Z_{D,i,t}$ is a binary random variable with possible states "no crack detection" (i.e. $Z_{D,i,t} = 0$), and "crack detection" (i.e. $Z_{D,i,t} = 1$). The inspection quality is described by an exponential probability of detection (POD) model with parameter ξ, in function of the crack depth d:

$$\Pr(Z = 1|D = d) = \mathrm{POD}(d) = 1 - \exp\left(-\frac{d}{\xi}\right) \tag{17}$$

4.1.3 Relation between component and system conditions

Failure of the i-th component after t time steps (equivalent to $n = n(t)$ stress cycles) occurs when the crack depth exceeds the critical value d_c, i.e. $\{E_{C,i,t} = 1\} = \{D_{i,t} \geq d_c\}$. If the component has not failed, it is assumed to have its full capacity.

In a Daniels system, due to the exchangeability of the components, the probability of having a system failure at time step t is a function only of the total number of component failures. Following section 3.3, to avoid a convergent connection between the $E_{C,i,t}$ and $E_{S,t}$, the cumulative number of component failures up to component i, $N_{f,1:i,t}$, is defined as follows:

$$N_{f,1:i,t} = \sum_{j=1}^{i} E_{C,j,t} = E_{C,i,t} + N_{f,1:i-1,t} \tag{18}$$

The relation between the component conditions $E_{C,i,t}$, $i = 1, \dots, N$ and the system condition $E_{S,t}$ defined in the general model of Figure 6 can be replaced by the network depicted in Figure 8. The complete DBN of the Daniels system is presented in Figure 9.

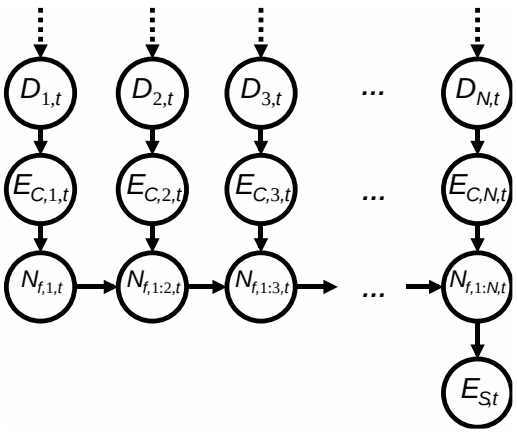

Figure 8. DBN model of the Daniels system condition. $N_{f,1:i,t}$ is the total number of component failures among the first i components at time t.

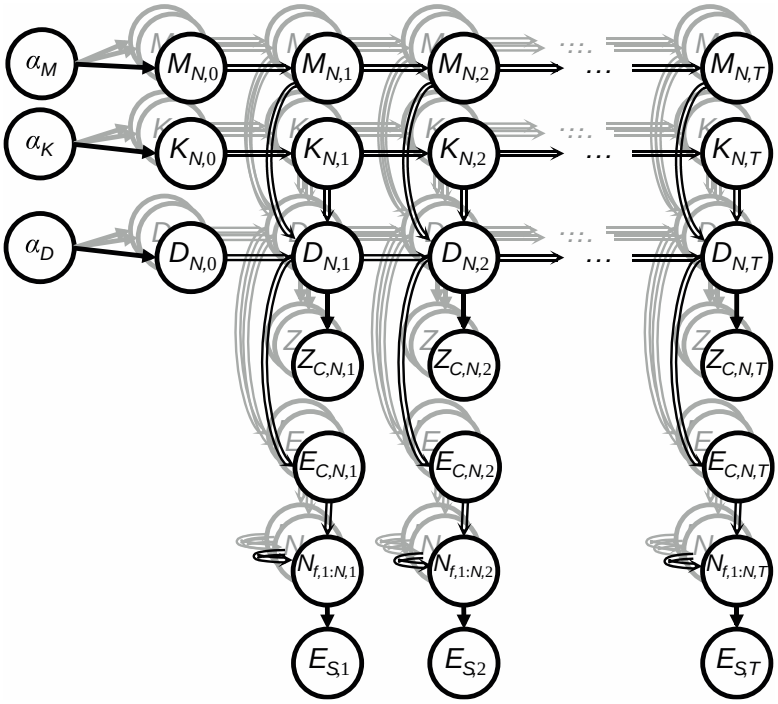

Figure 9. DBN of the Daniels system.

A Daniels system with $N = 10$ components and $T = 100$ time steps is investigated. The parameters of the fatigue deterioration model are summarized in Table 1 and the corresponding discretization scheme is presented in Table 2. Each time step corresponds to $\Delta n = 5 \cdot 10^6$ fatigue stress cycles. The correlation of fatigue parameters among components are $\rho_{D_0} = 0.5$, $\rho_M = 0.6$, and $\rho_K = 0.8$.

Table 1. Parameters of the fatigue deterioration model.

Random variable	Distribution	Mean	Std. deviation
α_{D_0}	Normal	0	1
α_K	Normal	0	1
α_M	Normal	0	1
$D_{0,i}$ (mm)	Exponential	1	1
$M_{0,i}$	Normal	3.5	0.3
$M_{t,i}$	$M_{t,i} = M_{t-1,i}$		
$ln\, C_{t,i}$	$\ln C_{t,i} = -3.34 M_{t,i} - 15.84$		
$K_{0,i}$	Lognormal	1.6	0.22
$K_{t,i}$	$K_{t,i} = K_{t-1,i}$		
λ_i	Deterministic	0.8	
d_C (mm)	Deterministic	50	
ξ (mm)	Deterministic	10	

Table 2. Discretization scheme.

Random variable	Number of states	Final interval boundaries
α_{D_0}, α_M, α_K	5	$\Phi^{-1}(0\text{: }0.2\text{: }1)$
D (mm)	80	$0, \exp\{\ln(0.01) : [\ln(50) - \ln(0.01)]/78 : \ln(50)\}, \infty$
M	20	$0, \ln\{\exp(2.2) : [\exp(4.8) - \exp(2.2)]/18 : \exp(4.8)\}, \infty$
K	20	$0, \{0.86 : (2.83 - 0.86)/18 : 2.83\}, \infty$

The load L is lognormal distributed with coefficient of variation $\delta_L = 0.25$, the capacities R_i, $i = 1, \ldots, 10$, are independent and normal distributed with $\delta_R = 0.15$ and the mean safety factor is $n\mu_{R_i}/\mu_L = 2.9$. The conditional probability of failure of the system given j failed components is computed according to Eq. (19) and is presented in Figure 10.

$$\Pr\left(E_{S,t} = 1 \middle| N_{f,1:N,t} = j\right) = \Pr\left(\sum_{i=1}^{n-j} R_i - L \leq 0\right) \tag{19}$$

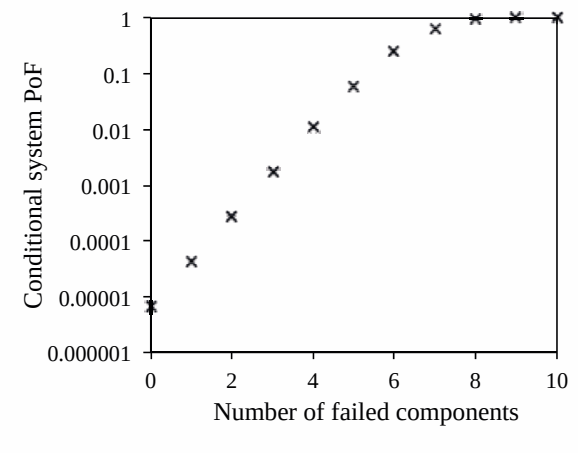

Figure 10. Probability of failure of the Daniels system conditional on the number of components with fatigue failures.

4.1.4 Results

For the unconditional case (i.e. without observations), the reliability index β calculated with the proposed inference algorithm is compared to the results obtained using MCS and MCMC for a single component (Figure 11) and the system (Figure 12). The reliability index is defined as $\beta = -\Phi^{-1}[\Pr(E = fail)]$, with Φ^{-1} being the inverse standard normal CDF.

A good agreement among the three methods is observed at the component level. At the system level, the difference between the probability estimates from the proposed DBN model and the

Monte Carlo methods is due to the discretization of the hyperparameters $\boldsymbol{\alpha}$ in the DBN. The relatively coarse discretization of α_{D_0}, α_M, and α_K using $m_{\alpha_{D_0}} = m_{\alpha_M} = m_{\alpha_K} = 5$ discrete states each (Table 2) leads to an underestimation of the correlation in the fatigue performance among components. This in turn leads to an overestimation of the system reliability in a redundant system, such as the Daniels system. The effect can be mitigated by increasing the number of discrete states for each hyperparameter, with an associated increase in computation time. Following Section 3.5, the computation time is linear with respect to m_α, the total number of states of the hyperparameters. Here it is $m_\alpha = m_{\alpha_{D_0}} \cdot m_{\alpha_M} \cdot m_{\alpha_K}$, and doubling the number of states of all hyperparameters would lead to an 8-fold increase in computation time. As shown later, the performance of the present discretization scheme in the case with observation is much better, and the accuracy is thus deemed acceptable.

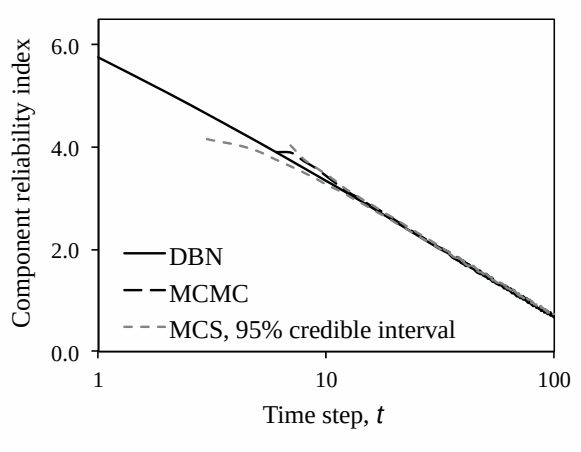

Figure 11. Reliability index of a single component.

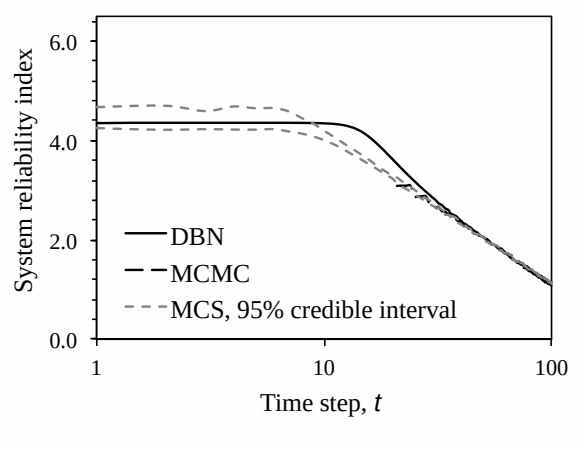

Figure 12. Reliability index of the Daniels system

To better understand the dependence among component deterioration, the correlation among crack depths D_i and D_j and among component failure events $E_{C,i} = 1$ and $E_{C,j} = 1$ is computed. These are obtained directly from the DBN or the Monte Carlo samples. Figure 13 shows the correlation between the crack depth of two components $D_{i,t}$ and $D_{j,t}$ using the proposed algorithm for DBNs, MCS and MCMC. As expected, the correlation is slightly underestimated by the DBN algorithm.

The dependence in fatigue performance among components is here due to inter-correlation of three parameters: a) the material parameter M, b) the stress parameter K, and c) the initial crack depth D_0. The correlation between the crack depths in two components at the beginning of the service life is dominated by the correlation in the initial crack depth D_0. The effect of the correlation in the material and stress parameters, M and K, increases with time.

The correlation between component failure events is shown in Figure 14. The correlation is low at the beginning of the service life, due to overall low probabilities of failure. In agreement with the above results, the DBN slightly underestimates the correlation.

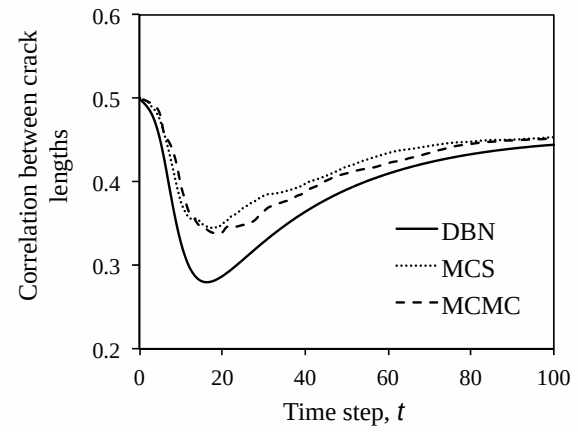

Figure 13 Correlation between the crack depths of two system components as a function of time, estimated using the DBN algorithm, MCS and MCMC.

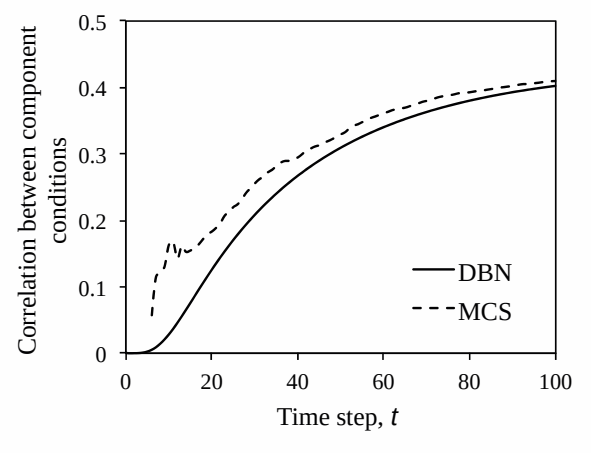

Figure 14. Correlation between the condition states E_C (i.e. failed/not failed) of two system components as a function of time, estimated using the DBN algorithm and MCS.

The relevant case for the DBN model is the conditional case, i.e. with the inclusion of inspections results. It is assumed that one component is inspected every $5 \cdot 10^7$ cycles, i.e. after every 10 time steps, without detecting any crack. The updated reliability index of the inspected component is considerably larger than in the unconditional case, due to the no-detection observation (Figure 15). This observation also affects the non-inspected components, due to the correlation defined by the hyperparameters (Figure 16). The reliability of the system is affected by the reliability of both the inspected and the non-inspected components (Figure 17). By inspection only one component every 10 time steps, and assuming that the inspections always result in a no-detection, the system reliability index at the end of the service life increases from 1.1 to 2.1.

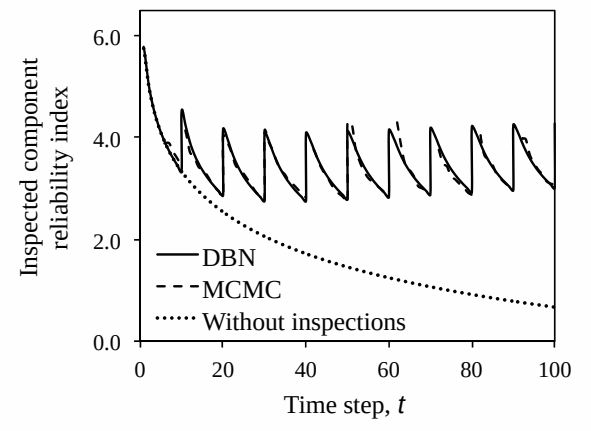

Figure 15. Reliability index of the inspected component after no detection of a crack at inspections every 10 time steps.

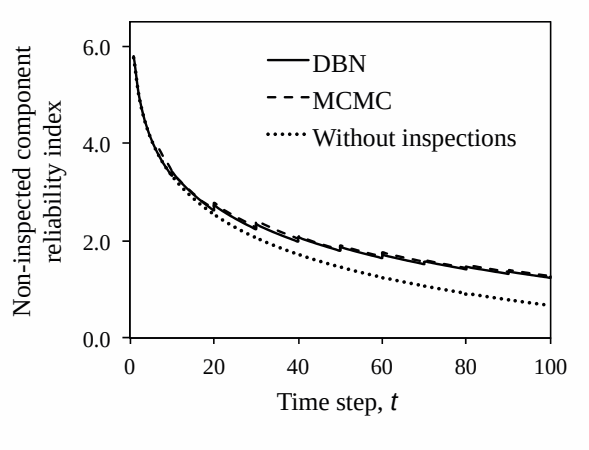

Figure 16. Reliability index of a non-inspected component given the no-detection outcome of the inspected component.

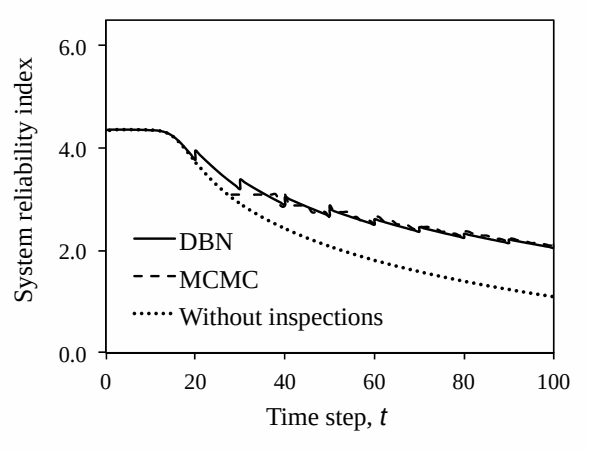

Figure 17. Reliability index of the system after no detection of a crack in all inspection times.

In Figures 15-17, the results of the DBN model are compared with results obtained by MCMC for verification. The results from the two algorithms match very well, and the slight differences observed in the unconditional case (Figure 12) are not seen here.

It is pointed out that the necessary computation time for the solution of the system DBN is orders of magnitudes lower than that for the applied standard MCMC algorithm. Additionally, the computation time of the forward-backward algorithm is not affected by the number of observations or the order of magnitude of the probability of failure, which is not the case of MCMC. If the number of system components increases, the computation time in both the forward-backward algorithm and MCMC increases linearly with number of components.

To demonstrate the efficiency of the DBN algorithm as the number of components and inspections is increased, we analyze a Daniels system with $N = 100$ components, in which 5 components are inspected every 10 time steps. The assumed inspection outcomes of the five

components are specified in Table 3. The probability of failure of the system using the forward-backward algorithm is shown in Figure 18. Since the inspection resulted in detection of multiple cracks, and no repairs are considered, the system reliability is lower after including the inspections. MCMC results are not computed for this case, due to the associated large computation times.

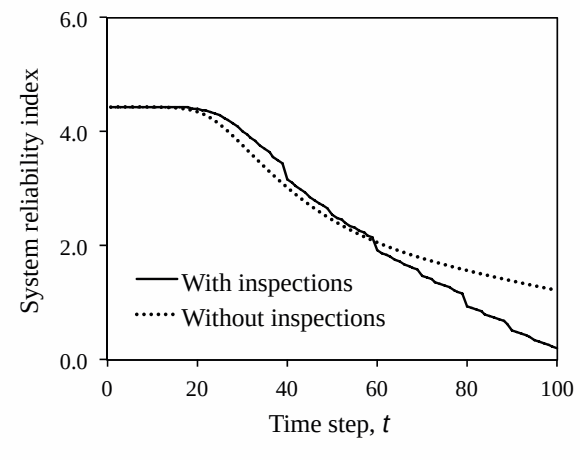

Figure 18. Reliability index of the Daniels system with 100 components for cases with and without inspections.

Table 3. Inspection outcomes of the Daniels system with 100 components.

	Inspection time step								
Component	10	20	30	40	50	60	70	80	90
1	×	✓	✓	✓	✓	✓	✓	✓	✓
2	×	×	×	✓	✓	✓	✓	✓	✓
3	×	×	×	×	×	✓	✓	✓	✓
4	×	×	×	×	×	×	×	✓	✓
5	×	×	×	×	×	×	×	×	×

✓: Detection; ×: No detection

4.2 Steel frame

The Zayas steel frame shown in Figure 19 is commonly used as a benchmark in structural analysis of steel offshore structures (Zayas et al. 1980). It consists of 23 tubular members with welded connections. The fatigue hotspots are located at the welded connections of the 13 horizontal and diagonal members. There are $N = 22$ fatigue hotspots, which represent the system components in the DBN model. The structure is loaded in horizontal direction by a concentrated force L at the upper left node of the structure and by gravity load. The details of the geometrical and material properties of the structure are described in (Schneider et al., under review).

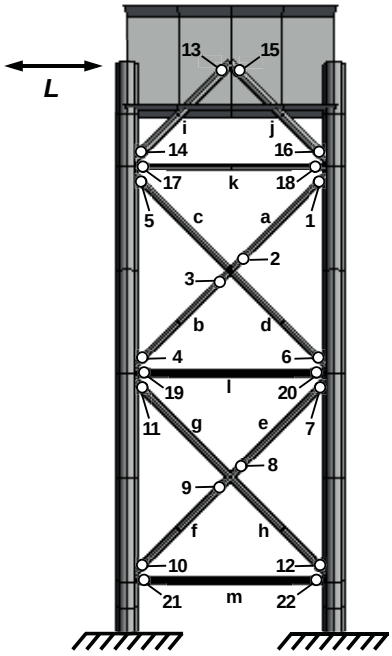

Figure 19. Zayas steel frame structure with 22 fatigue hotspots in 13 tubular members (a – m).

4.2.1 Deterioration model

For ease of presentation, fatigue deterioration in all hotspots of the Zayas frame structure is represented by the same model as used in section 4.1.1 with the parameters listed in Table 1. In a real structure, fatigue stresses will vary among hotspots. However, this has no impact on the computational demand and the accuracy of the reliability computations and the updating. As in example 1, a redistribution of fatigue stresses when some system components fail is neglected, i.e. $K_{i,t}$ is modeled as a time-invariant parameter.

4.2.2 Crack measurements as observations

In this example, measurements of crack sizes at the hot spots are included. To this end, the observation $Z_{i,t}$ conditional on $D_{i,t}$ is defined as

$$\Pr(Z_{i,t} = z | D_{i,t} = d) = f_\epsilon(z - d)$$

where f_ϵ is the normal probability distribution of the measurement error with zero mean and standard deviation $\sigma_e = 0.1\text{mm}$. The observation $Z_{i,t}$ is discretized with the same scheme as the crack depth $D_{i,t}$, with one additional state representing no detection. Note that the discretization of $Z_{i,t}$ has no effect on the computational demand.

4.2.3 Relation between hotspots, structural elements and system condition

To each of the structural elements, one or two fatigue hotspots are associated (Figure 19). The condition of hotspots and elements is modeled through the random variables E_h and E_e, respectively. It is assumed that an element fails if any of its hotspots fails, where a hotspot failure is defined according to section 4.1.3. Considering the number of structural members included in the Zayas frame, the total number of possible system configurations is $2^{13} = 8192$, which is still manageable. To estimate the probability of failure of the system, the ultimate capacity of the structure is obtained for each possible system configuration through a pushover analysis. The ultimate capacity of the structure when all components are intact is $2.8 \cdot 10^5$N. The condition of the system $E_{S,t}$ is defined as a child node of the system configuration and the extreme load L_t observed during time step t. The load L affecting the structure is assumed lognormal distributed with mean $4 \cdot 10^3$N and standard deviation $2 \cdot 10^4$N. The complete DBN model is shown in Figure 20.

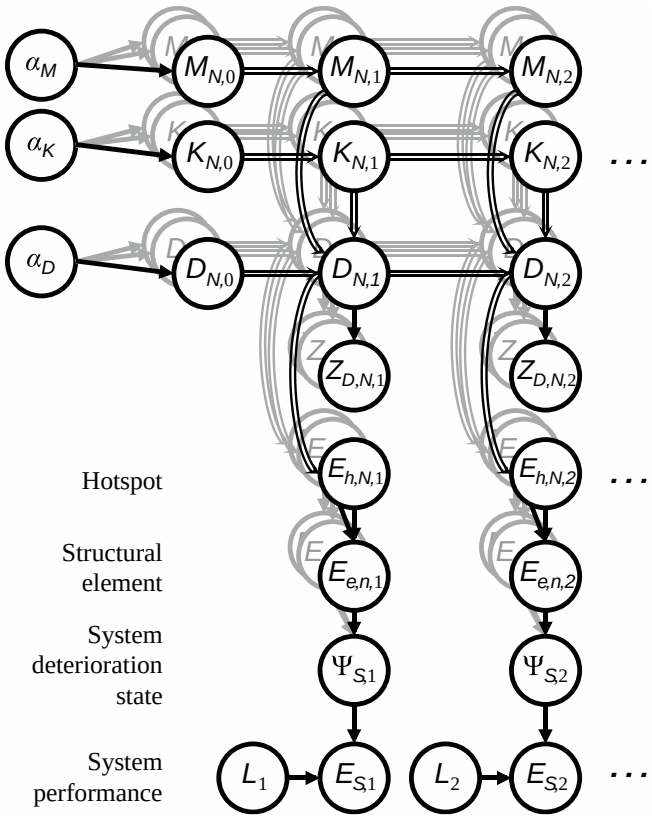

Figure 20. DBN of the Zayas frame.

4.2.4 Results

The accuracy of the proposed algorithm is compared to MCMC and MCS results. In the unconditional case, the three methods give consistent results for a single hotspot (Figure 21) and the system (Figure 22).

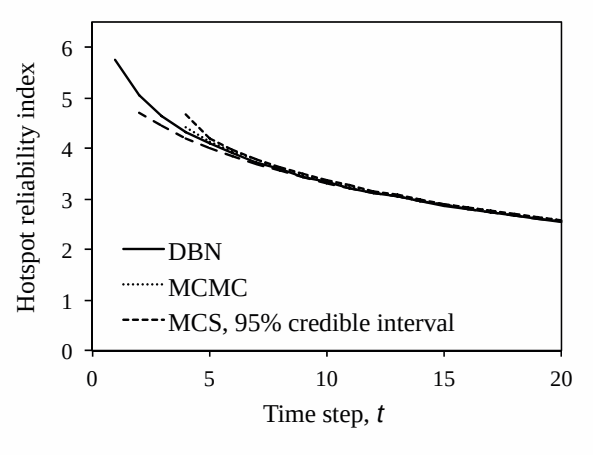

Figure 21. Reliability index of a single hotspot for the unconditional case (i.e. without inspection).

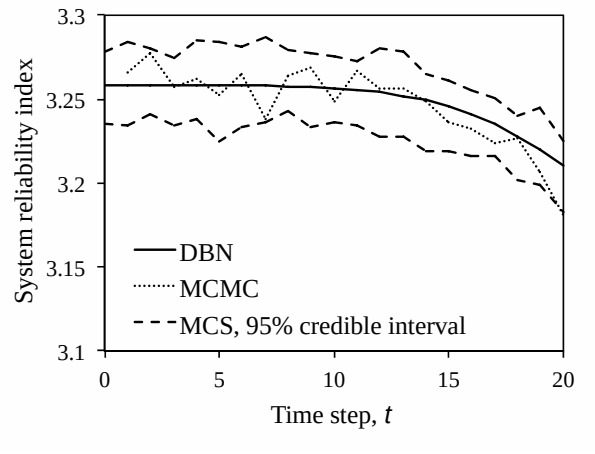

Figure 22. Reliability index of the system for the unconditional case (i.e. without inspection).

For the conditional case, it is assumed that hotspot 1 (in structural element 1) is inspected at time step $t = 10$. A crack of depth $Z_{D,1,10} = 3\text{mm}$ is measured, which should be compared to the expected crack depth before the observation of $\mathrm{E}\left[D_{1,10}\right] = 1.2\text{mm}$. Results are obtained using the algorithm described in Section 3.4 for the inspected hotspot (Figure 23), a non-inspected hotspot (Figure 24), and the system (Figure 25). When including crack measurements, MCMC using OpenBUGS has convergence issues and no reliability estimates are obtained.

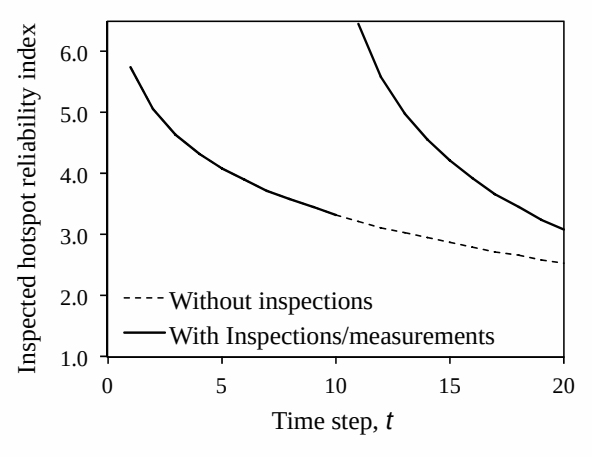

585

586 *Figure 23. Reliability index of the inspected hotspot.*

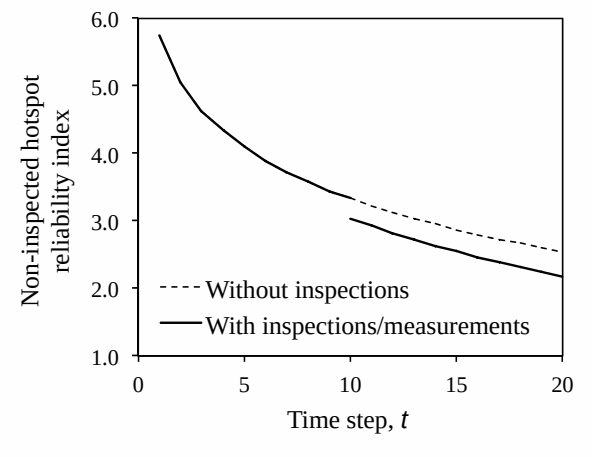

587

588 *Figure 24. Reliability index of a non-inspected hotspot for the conditional case (i.e. with inspection).*

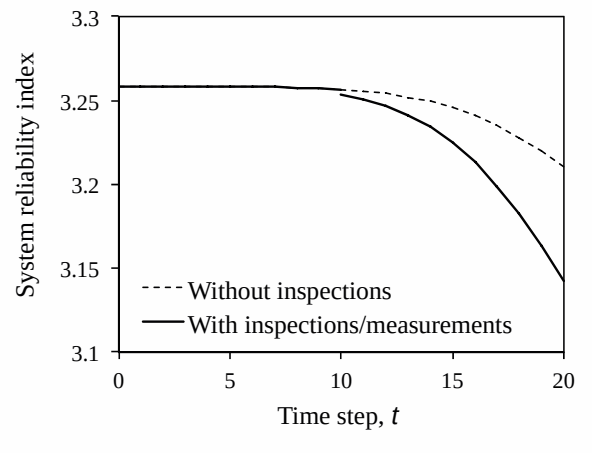

589

590 *Figure 25. Reliability index of the system for the conditional case (i.e. with inspection).*

591 Although the measured crack is larger than the expected crack depth for that hotspot, the
592 reliability of the inspected hotspot increases after the inspection due to the combination of two

factors: 1) the measurement of 3mm is considerably smaller than the critical crack length 50mm, 2) the measurement error is small, and the overall uncertainty on the crack length is reduced. However, because the measured crack is larger than the expected, the reliability indexes of the other components are reduced, and this leads to a reduction in the estimate of system reliability.

As stated earlier, increasing the number of observations does not affect the computation time of the proposed algorithm. To include an example with more inspection results, Figure 26 presents the reliability index of the system given multiple observations at hotspots 1 to 4 and time steps 10, 20, 30, and 40.

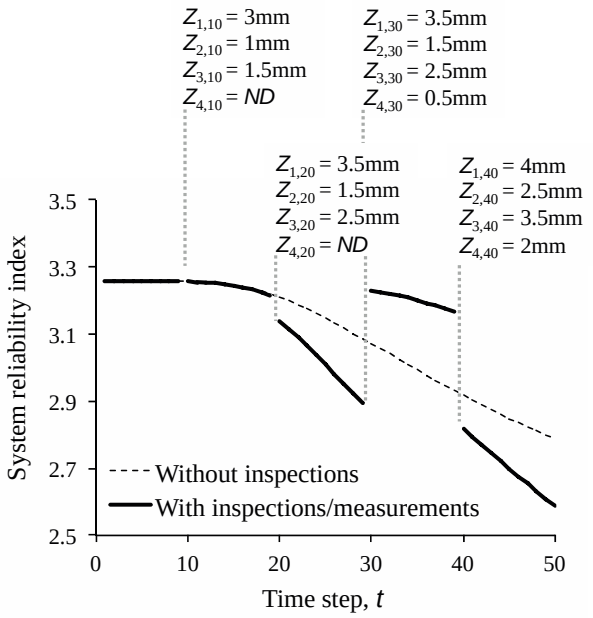

Figure 26. Reliability index of the system for the conditional case (i.e. with inspection) with observations from hotspots 1 to 4 at time steps 10, 20, 30 and 40. A measurement ND represents a no-detection case.

5 Discussion

We propose the use of a hierarchical DBN model for probabilistically representing deterioration in structural systems and for updating the probabilities and reliability when inspection and monitoring results are available. We also introduce an efficient algorithm for evaluating the hierarchical DBN. A major motivation for the use of the DBN in conjunction with the exact inference algorithm is its fast and robust computational performance. With the exception of the last step, the system deterioration model presented in Figure 6 can be solved with almost linear computational complexity with respect to the number of time steps and the number of

components. Importantly, the computation time is not affected by the number of inspection and monitoring outcomes included in the model. In addition, due to the hierarchical definition of the model, the proposed inference algorithm can be run in parallel for each component before and after the hyperparameters are updated. This part of the algorithm represents a considerable percentage of the total computation time, e.g. more than 90% for the Daniels system and 80% for the Zayas frame examples investigated in this paper.

For the last step, the updating of the system condition, a direct modeling of the structural system is in most cases prohibitively expensive for realistic structural systems, as this entails considering 2^N system configurations, with N being the number of affected components. Different application-specific modeling strategies for dealing with this issue are available. In some cases, as demonstrated in the numerical investigations, components can be grouped and it is sufficient to consider their cumulative effect on the system reliability. The DBN model of the system behavior can accommodate such a modeling. Alternatively, approximate models of system behavior may be applied, such as the model proposed in Straub and Der Kiureghian (2011), which requires only the marginal effect of component failure on the system reliability as an input. Finally, one might combine the proposed exact algorithm with sampling-based methods to be used in the last step. Samples of the correlated component behavior can be generated from the posterior distribution of the component states obtained with the DBN algorithm. This has not been investigated in this paper and further work is needed on finding efficient representation of structural system behavior with component deterioration failures. However, it is important to realize that the challenges associated with the system representation are independent of the algorithm used for performing the Bayesian updating of the system reliability.

The investigated examples demonstrate the advantages of the proposed inference algorithm over a standard MCMC algorithm. The former leads to computation times that are orders of magnitude lower. Although a direct comparison of computation time has only a limited value due to the difference in software used for their implementation, the difference in computational complexity is noticeable. In particular, the performance of MCMC deteriorates when increasing the amount and accuracy of inspection and monitoring results. With tailor-made MCMC algorithms, its performance could be significantly increased, but it will always vary with the data. In addition, current simulation-based methods (e.g. MCMC) are not well suited to estimate small probabilities of failure, even if recent developments are improving this (e.g. Straub and Papaioannou 2015, Schneider et al., under review).

The limitations of the proposed approach are related to the discretization of the continuous random variables. More specifically, the computational complexity is a linear or quadratic function of the number of states used for discretizing the random variables (Section 3.5). Therefore, the number of random variables that can be included explicitly in the DBN model is limited. While the deterioration model considered in this paper includes only four random variables, published state of the art models often include more random variables. Nevertheless, the problem is less critical as it may seem at first glance. The number of random variables can often be reduced by combining multiple random variables to a single random variable, as exemplarily shown in Straub (2009). In addition, in models with many random variables it is often possible to consider some as deterministic with limited loss of accuracy. Besides the need to limit the number of random variables, the second drawback of the proposed algorithm is the increased effort in pre-processing. The choice of the discretization scheme and its implementation lead to an increased effort by the analyst. For this reason, the DBN framework is mainly of use when computations have to be performed repetitively (e.g. multiple function evaluations to solve an optimization problem) and/or included in software. This is e.g., the case when analyzing portfolios of structures, or in the operational planning of inspections, monitoring, maintenance activities, and in near-real-time situations.

6 Conclusions

A hierarchical dynamic Bayesian to model the deterioration process in structural systems is proposed. The model includes the dependence among system components when assessing the effect of (partial) observations of system components on the probability of system failure. An efficient algorithm for performing Bayesian updating at the system level is provided, which operates recursively among components and time steps. The hierarchical definition of the components facilitates parallelizing the code to further reduce computation time. The accuracy and performance of the model is tested through two case studies. A comparison with Markov Chin Monte Carlo (MCMC) shows good agreement in the updated probabilities, with computation times that are orders of magnitude lower. A particular advantage is that the computational cost of the proposed algorithm is independent of the number of included inspection and monitoring results and of the magnitude of the probability of failure. This efficiency and robustness make the proposed algorithm suitable for integral planning and optimization of monitoring, inspection and maintenance activities in structural systems.

Acknowledgement

The authors thank Marcel Nowak for his support on the structural analyses of the Zayas frame. This work is supported by the Deutsche Forschungsgemeinschaft (DFG) through Grant STR 1140/3-1 and the Consejo Nacional de Ciencia y Tecnología (CONACYT) through Grant No. 311700.

References

Banerjee S., Carlin B.P., Gelfand A.E., (2015). Hierarchical modeling and analysis for spatial data, CRC Press, Second Edition.

Bensi M.T., Der Kiureghian A., Straub D., (2011). Bayesian network modeling of correlated random variables drawn from a Gaussian random field. Structural Safety, 33(6), pp. 317–332.

Brownjohn J.M.W., (2007). Structural health monitoring of civil infrastructure. Philosophical transactions of the Royal Society. Mathematical, Physical and engineering sciences, 365: 589–622.

Chang K.C., Chen H.D., (2005). Efficient inference for hybrid dynamic Bayesian networks. Proc. SPIE 5429, Signal Processing, Sensor Fusion, and Target Recognition XIII, 402.

Daniels H.E., (1945). The statistical theory of the strength of bundles of threads, Part I. Proc. Roy. Soc., A, 183(995), 405-435.

Ditlevsen O., Madsen H.O., (1996). Structural reliability methods, Wiley, New York.

Faber M.H., Engelund S., Sørensen J.D., Bloch A., (2000). Simplified and generic risk based inspection planning. Proc., 19th Offshore Mechanics and Arctic Engineering Conference, ASME.

Faber M.H., Straub D., Maes M.A., (2006). A computational framework for risk assessment of RC structures using indicators. Computer-Aided Civil and Infrastructure Engineering 21(3), 216-230.

Farrar C.R., Worden K., (2007). An introduction to structural health monitoring. Philosophical transactions of the Royal Society. Mathematical, Physical and engineering sciences, 365(1851): 303–315.

Frangopol D.M., Kallen M.J., Van Noortwijk J.M., (2004). Probabilistic models for life-cycle performance of deteriorating structures: review and future directions. Progress in Structural Engineering and Materials, 6(4): 197-212.

Gamerman D., Lopes H.F., (2006). Markov Chain Monte Carlo, stochastic simulation for Bayesian inference. 2nd Ed. Chapman & Hall/CRC, Florida, USA.

Gardiner C.P., Melchers R.E., (2003). Corrosion analysis of bulk carriers, Part I: operational parameters influencing corrosion rates. Marine Structures 16, 547–566.

Gollwitzer S., Rackwitz R., (1990). On the reliability of Daniels systems. Structural Safety, 7(2-4), 229–243.

Guedes Soares C., Garbatov Y., (1997). Reliability assessment of maintained ship hulls with correlated corroded elements. Marine Structures 10, pp. 629-653.

Hanea A., Kurowicka D., Cooke R., (2006). Hybrid method for quantifying and analyzing Bayesian belief nets. Quality and Reliability Engineering International 22(6), 613–729.

Hergenröder M, Rackwitz R, (1992). Maintenance strategy for RC-elements under normal outdoor exposure conditions. Bridge Rehabilitation. Proceedings of the 3rd International Workshop on Bridge Rehabilitation.

Jensen F.V., Nielsen T.D., (2007). Bayesian networks and decision graphs. Second Edition. New York, NY. Springer (Information Science and Statistics).

Kang W.H., Song J., (2010). Evaluation of multivariate normal integrals for general systems by sequential compounding. Journal of Structural Safety 32(1), pp 35–41.

Kang W.H., Song J., (2009). Efficient reliability analysis of general systems by sequential compounding using Dunnett-Sobel correlation model. Proc. 10th International Conference on Structural Safety and Reliability (ICOSSAR2009), Osaka, Japan.

Kim D.S., Ok S.Y., Song J., Koh H.M., (2013). System reliability analysis using dominant failure modes identified by selective searching technique. Reliability Engineering & System Safety, 119, 316-331.

Langseth H., Nielsen T.D., Rumí R., Salmerón A., (2009). Inference in hybrid Bayesian networks. Reliability Engineering and System Safety, 94(10), 1499–1509.

Lee Y.J., Song J., (2014). System reliability updating of fatigue-induced sequential failures. Journal of Structural Engineering, 140(3), 04013074-1~16.

Lin Y.K., Yang J.N., (1985). A stochastic theory of fatigue crack propagation. AIAA J., 23(1), 117-124.

Liu P.-L., Der Kiureghian A. (1986). Multivariate distribution models with prescribed marginals and covariances. Probabilistic Engineering Mechanics, 1(2), 105-112.

Lunn D., Spiegelhalter D., Thomas A., Best N., (2009) The BUGS project: Evolution, critique and future directions (with discussion), Statistics in Medicine, 28, 3049-3082

Luque J., Hamann R., Straub D., (2014). Spatial model for corrosion in ships and FPSOs. Proc. OMAE2014, San Francisco, CA.

Luque J., Straub D., (2015). Reliability analysis of monitored deteriorating structural systems with dynamic Bayesian networks. Proc. 12th International Conference on Applications of Statistics and Probability in Civil Engineering, Vancouver, Canada.

Maljaars J., Vrouwenvelder A.C.W.M., (2014). Probabilistic fatigue life updating accounting for inspections of multiple critical locations. International Journal of Fatigue 68, 24-37

Madsen H.O., Krenk S., Lind N.C., (1985). Methods of structural safety. Englewood Cliffs, NJ, Prentice Hall.

Madsen H.O., (1997). Stochastic modeling of fatigue crack growth and inspection. IN SOARES, C.G. (Ed.) Probabilistic Methods for Structural Design. Kluwer Academic Publishers. Printed in the Netherlands.

Maes M.A., (2003). Modelling infrastructure deterioration risks. International Journal of Modelling and Simulation 23/1, S. 43-51.

Maes M.A., Dann M., (2007). Hierarchical Bayes methods for systems with spatially varying condition states. Canadian Journal of Civil Engineering 34, pp. 1289- 1298

746 Maes M., Dann M., Breitung K., Brehm E., (2008). Hierarchical modeling of stochastic deterioration. Graubner,
747 Schmidt & Proske: Proceedings of the 6th International Probabilistic Workshop, Darmstadt.

748 Mahadevan S., Zhang R., Smith N., (2001). Bayesian networks for system reliability reassessment. Structural
749 Safety, 23(3), 231-251.

750 Malioka V., (2009). Condition indicators for the assessment of local and spatial deterioration of concrete structures.
751 Ph.D thesis, ETH Zürich, Switzerland.

752 Marquez D., Neil M., Fenton N., (2010). Improved reliability modeling using Bayesian networks and dynamic
753 discretization. Reliability Engineering and System Safety 95(4), 412–425.

754 Melchers R.E., (1999). Corrosion uncertainty modeling for steel structures. Constructional Steel Research, 52, 3-
755 19.

756 Memarzadeh M., Pozzi M., Kolter J.Z., (2014). Optimal planning and learning in uncertain environments for the
757 management of wind farms. ASCE J. of Computing in Civil Engineering, DOI: 10.1061/(ASCE)CP. 1943-
758 5487.0000390.

759 Moan T., (2005). Reliability-based management of inspection, maintenance and repair of offshore structures.
760 Structure and Infrastructure Engineering, 1(1), 33–62.

761 Moan T., Song R., (2000). Implications of inspection updating on system fatigue reliability of offshore structures.
762 Journal of Offshore Mechanics and Artic Engineering, 122, 173-180.

763 Murphy K.P., (2002). Dynamic Bayesian networks: Representation, inference and learning. Ph.D Thesis, Univ. of
764 California, Berkeley, Calif, 268.

765 Neil M., Tailor M., Marquez D., (2007). Inference in hybrid Bayesian networks using dynamic discretization.
766 Statistics and Computing 17(3), p. 219-233.

767 Nielsen J.S., Sørensen, J.D., (2014). Methods for risk-based planning of O&M of wind turbines. Energies, Vol.
768 7(10), 6645-6664.

769 Qin J., Faber M.H., (2012). Risk management of large RC structures within a spatial information system.
770 Computer-Aided Civil and Infrastructure Engineering, 27(6), 385-405.

771 Qin S., Cui W., (2003). Effect of corrosion models on the time-dependent reliability of steel plated elements.
772 Marine Structures 16, 15–34.

773 Raudenbush S.W., Bryk A.S., (2008). Hierarchical linear models, applications and data analysis methods. 2nd Ed.
774 SAGE Publications, Inc. California, USA.

775 Russell S.J., Norvig P., (2003). Artificial intelligence: A modern approach. 2nd Ed. Prentice-Hall, Englewood
776 Cliffs, N.J.

777 Schneider R., Fischer J., Bügler M., Nowak M., Thöns S., Borrmann A., Straub D., (2015). Assessing and updating
778 the reliability of concrete bridges subjected to spatial deterioration – principles and software implementation.
779 Structural Concrete, 16(3): 356-365.

780 Schneider R., Thöns S., Straub D. (under review): Reliability analysis and updating of structural systems with
781 subset simulation. Submitted to *Structural Safety*.

782 Shenoy P.P., West J.C., (2011). Inference in hybrid Bayesian networks using mixtures of polynomials.
783 International Journal of Approximate Reasoning, 52(5), 641-657

784 Stephens R.I., (2001). Metal fatigue in engineering. 2. ed. New York, NY, Wiley.

785 Stewart M.G., Mullard J.A., (2007). Spatial time-dependent reliability analysis of corrosion damage and the timing
786 of first repair for RC structures. Engineering Structures 29(7), 1457-1464.

787 Straub D., Malioka V., Faber M.H., (2009). A framework for the asset integrity management of large deteriorating
788 concrete structures. Structure and Infrastructure Engineering, 5(3), 199 - 213.

789 Straub D., (2009). Stochastic modeling of deterioration processes through dynamic Bayesian networks. Journal of
790 Engineering Mechanics, Trans. ASCE, 135(10), pp. 1089-1099.

791 Straub D., (2011a). Reliability updating with equality information. Probabilistic Engineering Mechanics, 26(2),
792 pp. 254–258.

793 Straub D., (2011b) Reliability updating with inspection and monitoring data in deteriorating reinforced concrete
794 slabs. Proc. ICASP11, Zürich, Switzerland.

795 Straub D., Der Kiureghian A., (2011). Reliability acceptance criteria for deteriorating elements of structural
796 systems. Journal of Structural Engineering, Trans. ASCE, 137(12): 1573–1582.

797 Straub D., Der Kiureghian A. (2010). Bayesian network enhanced with structural reliability methods. Part A:
798 Theory & Part B: Applications. Journal of Engineering Mechanics, Trans. ASCE, 136(10), 1248-1270.

799 Straub D., Faber M.H., (2005). Risk based inspection planning for structural systems. Structural Safety, 27(4): pp
800 335-355.

801 Straub D., Papaioannou I., (2015). Bayesian updating with structural reliability methods. ASCE Journal of
802 Engineering Mechanics 141(3), 04014134.

803 Swanson L., (2001). Linking maintenance strategies to performance. Int. J. Production Economics, 70: 237–244.

804 Tang W., (1973). Probabilistic updating of flaw information. Journal of Testing and Evaluation, 1, 459-467

805 Thoft-Christensen P., Murotsu Y., (1986). Application of structural systems reliability theory, Springer.

806 Thoft-Christensen P., Sørensen J. D., (1987). Optimal strategy for inspection and repair of structural systems. Civil
807 Engineering Systems, 4(2), 94-100.

808 Vrouwenvelder T., (2004). Spatial correlation aspects in deterioration models. Proc., 2nd Int. Conf. Lifetime-
809 Oriented Design Concepts, F. Stangenberg, ed., Ruhr-Universität Bochum, Germany.

810 Weber P., Medina-Oliva G., Simon C., Iung B., (2010). Overview on Bayesian networks applications for
811 dependability, risk analysis and maintenance areas. Engineering Applications of Artificial Intelligence,
812 International Federation of Automatic Control, 2012, 25(4), pp.671-682.

813 Wells T., Melchers R.E., (2014). An observation-based model for corrosion of concrete sewers under aggressive
814 conditions. Cement and Concrete Research, 61, 1–10.

815 Zayas V., Mahin S.A., Popov E.P., (1980). Cyclic inelastic behavior of steel offshore structures. Univ. of
816 California, Berkeley, Earthquake Engineering Research Center Report No. UCCB/EERC-80/27.

817 Zwirglmaier K., Straub D.: A discretization procedure for rare events in Bayesian networks. *Reliability
818 Engineering & System Safety*, under review.